Applied Chemical Engineering (2026) Volume 9 Issue 1 ISSN: 2578-2010 (O)
doi: 10.59429/ace.v9i1.5838

ORIGINAL RESEARCH ARTICLE

Low-Carbon design of offshore wind turbine foundations and optimization of multi-energy complementary new energy systems based on smart grid collaboration

Ningfeng Huang*

School of Engineerring, The University of Western Australia, 6009 Perth, Australia

***Corresponding author:** Ningfeng Huang, 24290489@uwa.edu.au

ABSTRACT

Offshore wind power, as a key clean energy in the energy transition, has significant advantages in resource abundance and stability. However, current offshore wind turbine foundation designs face high carbon emissions, and the variability of offshore power generation easily increases the operational costs of the power system. In the design of basic structures, the chemical properties of materials have a significant impact on carbon emissions, costs and performance. However, current research lacks in-depth exploration of common directions in applied chemistry such as materials, reactions and chemical processes. This study proposes a low-carbon design of offshore wind turbine foundations and an optimization model of multi-energy complementary new energy systems based on smart grid collaboration. The experimental results indicated that after optimization with the proposed algorithm, the carbon emissions reached 2087.2 tons. The average cost of the proposed model is 7531.67 dollars, and the power balance constraint during peak load periods is satisfied at a rate of 98.51%. The supply insufficiency during low load periods is only 0.72%, and both curtailment rate and unit output exceedance occurrences are improved. These findings suggest that the proposed model was capable of achieving an effective balance between economic efficiency and environmental performance of offshore wind turbine foundations and promote low-carbon and efficient development of offshore wind power and new energy systems.

Keywords: smart grid; offshore wind power; foundation design; multi-energy complementarity; new energy systems

ARTICLE INFO

Received: 25 November 2025
Accepted: 15 December 2025
Available online: 20 January 2026

1. Overview

Offshore wind power, as a clean energy with great potential, has gradually become an important part of the energy transition. Offshore wind energy has characteristics of abundant resources, stability, and relatively high energy density. However, current offshore wind turbine foundations still face high cost and high emission issues during design and construction[1]. At the same time, the intermittency and variability of offshore power generation make it difficult to accurately predict and stably control the generation capacity of the power system, thereby increasing operational costs[2]. Smart Grid (SG), as an important infrastructure in the energy field, provides powerful data collection, analysis, and real-time control capabilities[3]. During the design stage of wind power infrastructure, it is necessary to simultaneously consider the coupling relationship between material chemical properties and engineering parameters, to extend the service life of the infrastructure and reduce carbon emissions. The Whale Optimization Algorithm (WOA) can break through the limitations of

traditional engineering optimization and incorporate material chemical indicators into the optimization objectives, achieving synchronous optimization of infrastructure parameters and material chemistry[4]. Particle Swarm Optimization (PSO) can optimize the dispatch of multi-energy complementary new energy systems through particle swarm search[5]. Model Predictive Control (MPC) can generate real-time operational strategies for each energy unit based on PSO results, ensuring that the power system meets device constraints and grid interaction limits while reducing operational costs and carbon emissions [6]. Therefore, this study optimizes offshore wind turbine foundation design based on the combination of SG and WOA, and further optimizes multi-energy complementary new energy systems based on PSO and MPC. The innovation of this study lies in proposing an improved WOA for low-carbon foundation design combined with smart grid to construct an optimization algorithm. At the same time, a coordinated scheduling framework based on PSO and MPC is established for multi-energy complementary new energy systems, achieving an integrated low-carbon technology pathway.

2. Research content

(1) The research first addressed the issues of insufficient initial population diversity and the tendency to get trapped in local optima in the traditional Whale Optimization Algorithm (WOA) in the design of offshore wind power infrastructure. It introduced a chaotic reverse learning strategy to construct an improved Whale Optimization Algorithm. Then, it generated chaotic variables with uniform distribution characteristics through Logistic chaotic mapping and combined the reverse learning mechanism to build a merged selection mechanism for the initial population and the reverse population, enhancing the ability of the population to cover the high-dimensional solution space. Through the fitness function, it quantified the carbon emissions and costs of the entire life cycle of the infrastructure and optimized the low-carbon economic design scheme that met the structural safety constraints.

(2) A PSO-MPC collaborative scheduling algorithm was constructed by integrating PSO and MPC. The particle position vector was set as the hourly output of energy units such as wind power, photovoltaic power, and gas turbines. Through the individual and global optimal learning mechanisms of PSO, the global optimization of high-dimensional scheduling parameters was achieved, avoiding the trap of local optima. Based on the real-time data of the intelligent power grid, a discrete state space model was constructed, and the prediction error was dynamically corrected to generate real-time scheduling strategies adapted to the fluctuation of output, ensuring the power balance and equipment constraints of the system.

(3) With the intelligent power grid as the core data hub and the collaborative control node, an integrated optimization model was constructed to achieve deep collaboration between the design of offshore wind power infrastructure and the scheduling of multi-energy complementary systems. The infrastructure design module received data such as marine environment, geological conditions, and equipment parameters from the intelligent power grid, and through the improved WOA algorithm, it output a foundation structure scheme that balanced low-carbon, economy, and safety. It also fed back parameters related to the stability of wind power output to the power grid hub. The multi-energy complementary scheduling module, based on real-time load data from the intelligent power grid, the predicted output data of new energy, and the characteristic parameters of the infrastructure, completed the allocation and dynamic scheduling of energy unit outputs through the PSO-MPC algorithm, forming a collaborative mechanism of two-way feedback between design and scheduling, and achieving a full-process low-carbon and efficient operation.

(4) Using the marine and geological exploration data of a certain offshore wind farm in southern China, the historical operation data of a provincial power grid, and the measured data of a multi-energy complementary new energy system on a southern island as experimental samples. Two types of comparative experiments were set up to verify the optimization effect of the foundation structure optimization algorithm

in terms of the weight of the foundation structure and the total cycle carbon emissions, as well as the performance of the integrated model in four dimensions of low-carbonity, economy, stability, and accuracy.

3. Low-carbon design of offshore wind turbine foundations and optimization of multi-energy complementary new energy systems

3.1. Low-carbon design optimization algorithm for offshore wind turbine foundations

The core of low-carbon design for offshore wind power foundation structures lies in achieving multi-objective optimization of carbon emissions, costs, and material performance throughout the entire life cycle of the foundation structure, while meeting the safety constraints of the structure[7]. The life cycle includes stages such as material production, transportation, construction, operation, maintenance, and recycling. The carbon emissions and costs in each stage are closely related to the chemical composition and reaction characteristics of the materials. Among them, the concrete and steel materials of the basic structure are important components of the optimization target. The concrete material achieves this by adjusting the ratio of cement to anti-fouling admixtures to control the rate and product of hydration reactions, ensuring strength while reducing the amount of cement used. The steel material achieves this by adding alloy elements to adjust the chemical composition of the steel, increasing the yield strength and corrosion resistance. The Whale Optimization Algorithm (WOA) mimicked three primary foraging strategies of whales—prey encirclement, bubble-net attack, and random search—to perform the optimization process. The position of each whale in the search space represents a combination solution of engineering parameters and chemical indicators, and it moved toward the optimal one by continuously updating its position. The position updating equation is shown in Equation (1)[8].

$$\begin{cases} X(t+1) = X'(t) - A \times D \\ D = C \times X'(t) - X(t) \\ C = 2 \times r \\ A = 2a \times r - a \end{cases} \tag{1}$$

In Equation (1), t represents the iteration, D represents the distance between solutions, X is the current position of the solution, A and C are the step lengths of the whale's movement, r is a random number between 0 and 1, and a represents the convergence factor that balances global and local search. Its calculation equation is shown in Equation (2)[9].

$$a = 2 - \frac{2 \times t}{T_{\max}} \tag{2}$$

In Equation (2), $T_{\max}$ represents the maximum iteration. The bubble-net attack simulates the spiral movement of whales when approaching prey. When $0 \le A \le 1$ is met, the whale contracts the encircling circle, and its position is updated in a spiral path to perform a fine search in the optimal region. The position updating equation is shown in Equation (3).

$$\begin{cases} X(t+1) = D' \cdot e^{bl} \cdot \cos(2\pi l) + X', p < 0.5 \\ X(t+1) = X'(t) - A \times D, p > 0.5 \\ D' = X'(t) - \hat{X}(t) \end{cases} \tag{3}$$

In Equation (3), p is the random number generated by the whale individual, b is the spiral shape constant, and l represents a random number between −1 and 1. When the current position of an individual is far from the optimal solution, the whale performs a random search to enhance global exploration ability. The position updating equation is shown in Equation (4)[10].

$$\begin{cases} X(t+1) = X_{rand} - A \cdot D \\ D = C \times X_{rand} - X \end{cases} \tag{4}$$

In Equation (4), X_{rand} represents the position of a randomly selected individual in the population. Although the traditional WOA shows certain optimization ability, it usually adopts random initialization of the population, which easily causes individuals to cluster in local regions of the search space and limits the exploration of the high-dimensional design space of offshore wind turbine foundations. Therefore, a chaotic reverse learning-based initialization method was incorporated to create a chaotic initial population with enhanced diversity. The chaotic and reverse populations are sorted and selected, and the individuals with better fitness are used as the initial population to improve optimization efficiency. The optimization process of offshore wind turbine foundation design based on Chaos Whale Optimization Algorithm (CWOA) is shown in **Figure 1**.

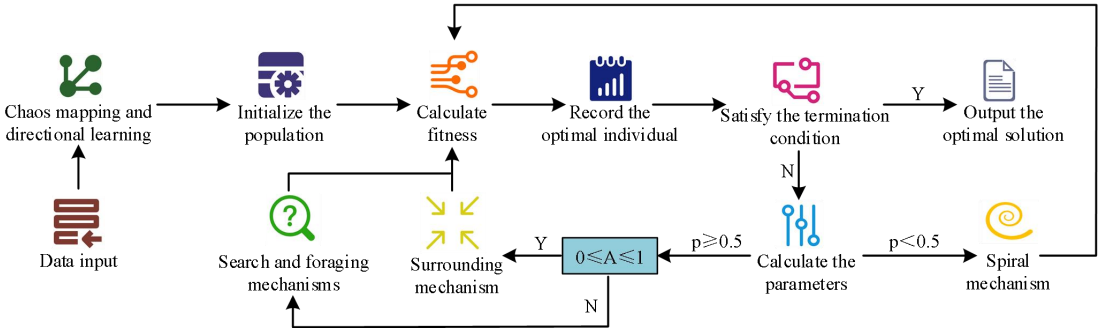

Figure 1. CWOA infrastructure design optimization process (Icon source from: Iconpark.oceanengine.com).

As shown in **Figure 1**, after the smart grid data and infrastructure data are input, they are first processed through chaotic mapping and reverse learning to generate the initial population covering the engineering and chemical dimensions. Then, the population fitness is calculated, the optimal individual is determined, and the parameters are calculated during the iteration. The individual positions are updated according to mechanisms such as enclosing, spiraling, and random search. During the iterative process, it is necessary to simultaneously verify that the solution meets the constraints of marine loads and geological bearing capacity at the engineering level, and the constraints of material corrosion resistance and recyclability at the chemical level. This process continues until a basic structure solution that is low-carbon, economical, safe, and long-lasting is achieved, and then the corresponding design plan is output. The expression of chaotic mapping is shown in Equation (5).

$$y_{i+1,d} = \begin{cases} 2y_{id}, y_{id} < 0.5 \\ 2(1 - y_{id}), y_{id} \geq 0.5 \end{cases} \tag{5}$$

In Equation (5), y represents the chaotic variable value of the individual, i represents the dimension index, and d represents the individual number. The initial population was generated through chaotic mapping, after which the corresponding reverse population was computed, as presented in Equation (6).

$$OX_{id} = X_{\min d} + X_{\max d} - [X_{\min d} + y_{id} \cdot (X_{\max d} - X_{\min d})] \tag{6}$$

In Equation (6), OX_{id} represents the reverse population. The original and reverse populations were combined to create a new population, from which the individuals with the highest fitness were chosen as the initial population. This allows the algorithm to find better solutions within a more uniformly distributed population, thereby accelerating convergence. The fitness function should take into account both engineering indicators and chemical indicators, and its expression is shown as Equation (7).

$$\hat{F} = \omega_1 \cdot \frac{W}{W_0} + \omega_2 \cdot \frac{C'}{C_0} + \omega_3 \cdot (1 - \frac{R}{R_0}) + \omega_4 \cdot (1 - \frac{S}{S_0}) \tag{7}$$

In Equation (7), $\hat{F}$ represents the fitness value, W and W_0 respectively represent the base structure weight and the weight of the traditional scheme, C' and C_0 respectively represent the carbon emission during the entire life cycle of the material and the carbon emission of the traditional scheme, R and R_0 respectively represent the material corrosion resistance score and the target corrosion resistance score, S and S_0 respectively represent the material recovery rate and the target recovery rate, and ω_1, ω_2, ω_3 and ω_4 are the weight coefficients.

3.2. Design of optimization model for multi-energy complementary new energy systems

CWOA achieves the optimization of carbon emissions and cost over the entire life cycle of offshore wind turbine foundations and establishes coordination between the foundation and SG at the design stage. The multi-energy complementary new energy system needs to address issues such as the intermittency of new energy outputs, multi-device coordinated scheduling, and system power balance[11]. Although MPC can handle dynamic changes in the power system through rolling optimization, it easily falls into local optima when optimizing high-dimensional energy scheduling parameters[12]. PSO treats the power output of wind, photovoltaic, and gas turbine units in different time periods as particle position vectors. By utilizing information from each particle's personal best position and the global best position within the solution space, PSO prevented convergence to local optima[13]. At the same time, it can incorporate parameters such as the chemical reaction efficiency of the energy storage materials and the aging rate of the equipment materials into the constraints of the particle position vector, thereby enhancing the practicality of the scheduling strategy. Therefore, this study combines MPC and PSO to construct a predictive optimization algorithm (PSO-MPC) that provides accurate operational strategies for energy units in multi-energy complementary systems. The process is shown in **Figure 2**.

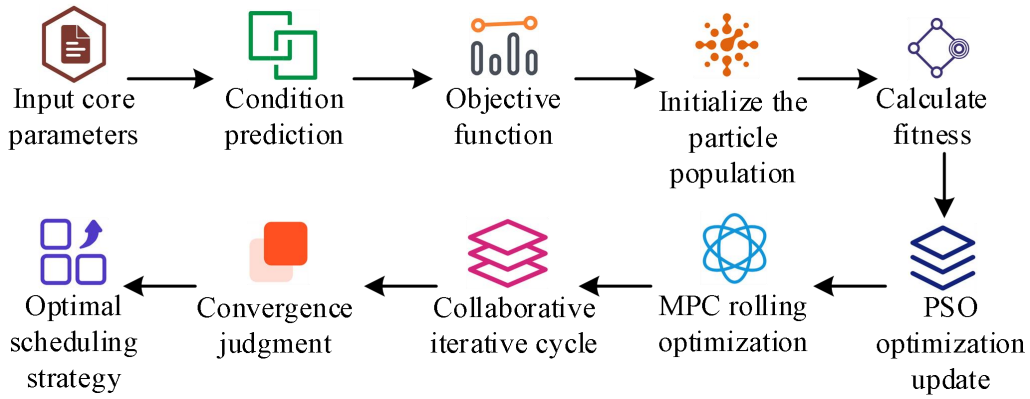

Figure 2. Schematic diagram of the PSO-MPC processing process (Icon source from: Iconpark.oceanengine.com).

As shown in **Figure 2**, in the PSO-MPC algorithm process, SG and system device parameters are first input to build a rolling prediction model using MPC, defining multi-objective optimization goals. Then, the PSO population is initialized, with energy unit outputs in each time period serving as particle position vectors. The fitness is calculated, and both the individual and global best positions are determined. PSO updates the particle positions through iteration, while MPC corrects the prediction error based on measured data. When convergence is reached, the optimized real-time scheduling strategy for energy units is output. During this process, MPC first constructs the discrete state-space model of the system, as shown in Equation (8)[14].

$$\begin{cases} x(k+1) = \hat{A}x(k) + B_u u(k) + B_{\hat{c}}\hat{c}(k) + B_d d(k) \\ \hat{y}(k) = \tilde{C}x(k) \end{cases} \tag{8}$$

In Equation (8), k is the time index, $\hat{A}$ represents the system dynamic matrix, B_u represents the control input matrix, u indicates the control input variable, $B_{\hat{c}}$ represents the matrix of chemical properties influence, $\hat{c}$ represents the chemical property parameters of the material, B_d represents the disturbance input matrix, d represents measurable external disturbances, $\hat{y}$ represents the system output vector, and $\tilde{C}$ represents the output matrix. The PSO then iteratively searches for the optimal power output strategy, and its updating equation is shown in Equation (9)[15].

$$\begin{cases} v_{i'd'} = \omega \cdot v_{i'd'} + c_1 \cdot r_1 \cdot (p_{i'd'} - x_{i'd'}) + c_2 \cdot r_2 \cdot (g_{d'} - x_{i'd'}) \\ x_{i'd'} = x_{i'd'} + v_{i'd'} \end{cases} \tag{9}$$

In Equation (9), v_{id} is the current velocity of particle i' in the d' dimension, ω is the inertia weight, $p_{i'd'}$ represents the individual best position, $g_{d'}$ represents the global best position of the population in the d' dimension. In summary, the PSO-MPC algorithm integrates PSO and MPC through coordinated optimization based on real-time data provided by SG. It optimizes power balance and coordinated scheduling of the multi-energy complementary new energy system while adapting to the intermittency of new energy, ensuring stable system operation. Therefore, this study constructs a low-carbon design and optimization model for offshore wind turbine foundations and multi-energy complementary new energy systems based on CWOA and PSO-MPC (CWOA-PSO-MPC). The structural schematic diagram is shown in **Figure 3**.

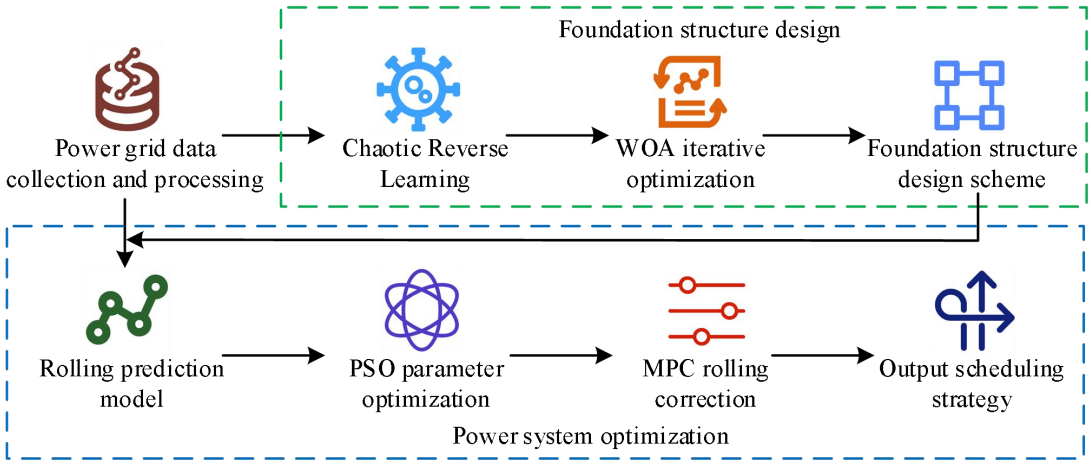

Figure 3. CWOA-PSO-MPC optimization model operation flow chart (Icon source from: Iconpark.oceanengine.com).

As shown in **Figure 3**, in the CWOA-PSO-MPC model, SG serves as the core data hub and coordination control node. SG inputs data such as marine environment, geological conditions, and equipment parameters, and first generates an initial population covering the high-dimensional solution space through chaotic reverse learning. WOA then iteratively searches for the optimal solution while verifying its feasibility under constraints such as marine load and geological bearing capacity. The final output is a foundation design scheme that balances low-carbon and economic performance. At the same time, SG receives feedback on the vibration resistance and stability of the foundation, providing data on wind power output stability for subsequent scheduling. On the multi-energy complementary system side, after receiving real-time load and predicted new energy output data from SG and foundation parameters from CWOA, MPC constructs a rolling prediction model with multiple future scheduling periods to clarify optimization goals such as power balance and equipment output limits. PSO converts the output of each energy unit in different time periods into particle position vectors and iteratively searches for the global optimal output combination

in the solution space. Finally, MPC continuously updates the scheduling strategy using real-time system operation data and outputs dynamic scheduling commands. This process stabilizes new energy output fluctuations, ensures stable operation of the system across all time periods, and realizes deep coordination between foundation design and multi-energy complementary scheduling.

4. Performance validation of low-carbon design and system optimization model

To verify the performance of the PSO-MPC model for low-carbon design of offshore wind turbine foundations and optimization of multi-energy complementary new energy systems, the study first analyzed the performance of the CWOA optimization algorithm for offshore wind turbine foundation design. The experimental system used Windows 10, an Intel Core i5-12400F@2.5GHz CPU, and an NVIDIA RTX3080 GPU (10GB). The experiment optimized the top-supported composite bucket foundation of an offshore wind farm in southern China using marine and geological data from a survey dataset and historical data from a provincial power grid enterprise. The study compared CWOA with Gray Wolf Optimization (GWO), Firefly Algorithm (FA), and Artificial Bee Colony (ABC). The study tested the design optimization results of weight and total cumulative carbon emissions for the four algorithms. Each algorithm ran independently 40 times, and the average of the best results was recorded. The convergence curves of weight and total cumulative carbon emissions are shown in **Figure 4**.

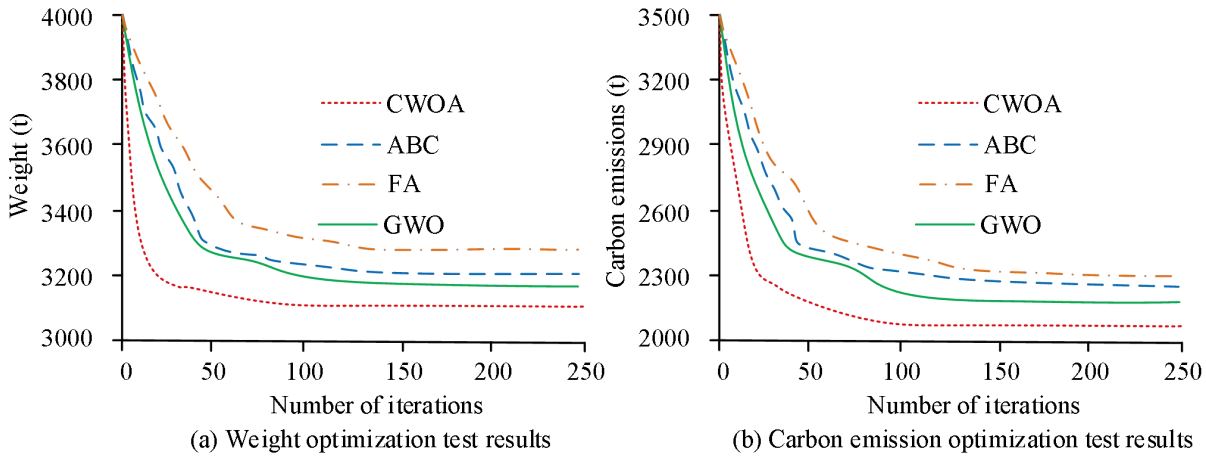

Figure 4. Weight and carbon emissions convergence curve results.

In **Figure 4(a)**, in the early stage of iteration, the weights of all four algorithms decreased rapidly, but the decline rate of CWOA was significantly faster. When the number of iterations reached 100, CWOA entered the convergence stage first, and the weight stabilized at 3169.3 tons. As shown in **Figure 4(b)**, when the number of iterations reached 100, the total cumulative carbon emissions of CWOA were 2087.2 tons, and the carbon emission curve gradually converged. In contrast, the other algorithms required further iterations to converge, and their final total carbon emissions were clearly higher than those of the proposed algorithm. These results indicated that CWOA overcame the problems of local optima and low efficiency and showed excellent performance in optimizing the top-supported composite bucket foundation of offshore wind power. After verifying the performance of CWOA, the study tested the performance of the CWOA-PSO-MPC model. The model was compared with GWO-PSO-PID (which combined GWO, PSO, and Proportional-Integral-Derivative Control), ABC-GA-LQR (which combined ABC, Genetic Algorithm, and Linear Quadratic Regulator), and FA-SA-FLC (which combined FA, Simulated Annealing, and Fuzzy Logic Control). The experiment used Python 3.8, and the control algorithm was implemented using Control 0.9.3. The study selected a multi-energy complementary new energy system on a southern Chinese island to test

the average daily operation cost and power balance constraint satisfaction rate of the four models. The test results are shown in **Figure 5**.

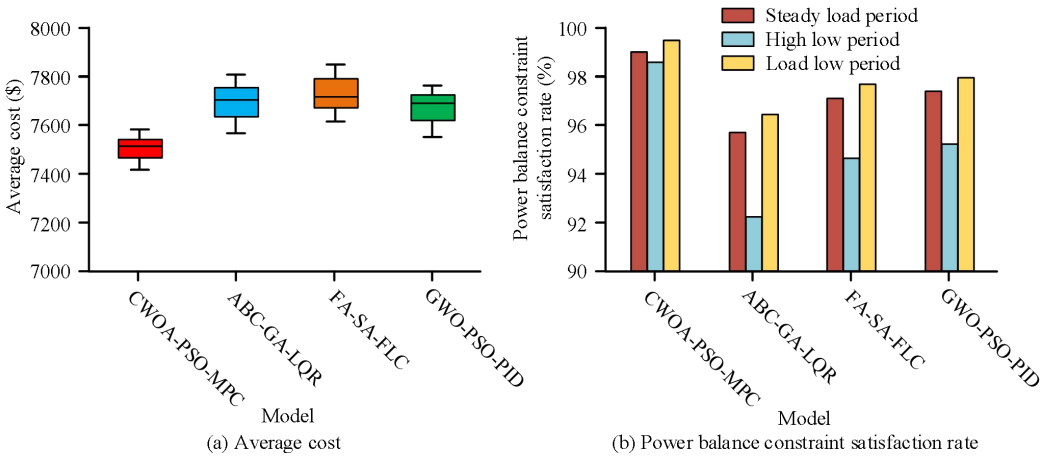

Figure 5. Average cost and power balance constraint satisfaction results.

As shown in **Figure 5(a)**, the average daily operation cost of the CWOA-PSO-MPC model was 7531.67 dollars, which was 215.39 dollars and 246.51 dollars lower than those of the ABC-GA-LQR model and the FA-SA-FLC model, respectively. As shown in **Figure 5(b)**, the CWOA-PSO-MPC model achieved a 98.51% power balance constraint satisfaction rate during peak load periods, which was 6.23% and 3.34% higher than those of the ABC-GA-LQR model and the GWO-PSO-PID model, respectively. During stable load periods, the CWOA-PSO-MPC model achieved a 99.26% satisfaction rate. The study then tested the Pearson correlation coefficients between the predicted new energy output ratios and the manually measured data for the CWOA-PSO-MPC model. The results are shown in **Figure 6**.

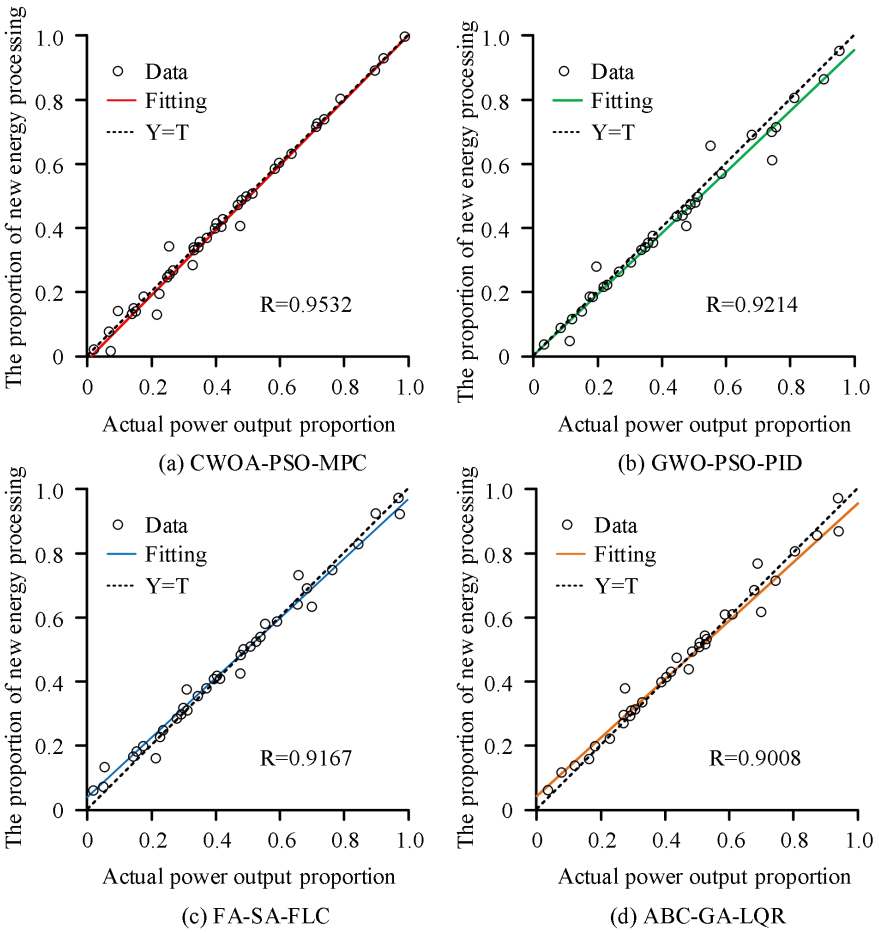

Figure 6. Comparison of Pearson coefficient test results.

In **Figure 6(a)**, the CWOA-PSO-MPC model achieved an excellent fitting performance, with a high degree of alignment between data points and the fitting curve, and the correlation coefficient reached 0.9532. In **Figure 6(b)**, the correlation coefficient of the GWO-PSO-PID model was 0.9214, which was 0.0318 lower than that of the proposed model. In **Figure 6(c)**, the correlation coefficient of the FA-SA-FLC model was 0.9167, which was also lower than that of the proposed algorithm. In **Figure 6(d)**, the correlation coefficient of the ABC-GA-LQR model decreased by 0.0524 compared with that of the CWOA-PSO-MPC model. These results indicated that the CWOA-PSO-MPC model predicted the new energy output ratio with higher accuracy. To further demonstrate the performance of the CWOA-PSO-MPC model, the study tested the curtailment rate, power shortage rate, and the number of unit output exceedances for the four models under high-load and low-load conditions. The test results are shown in **Table 1**.

Table 1. Comparison of test results of several comprehensive indicators.

Electric load	Model	Curtailment rate (%)	Power supply shortage rate (%)	number of unit output limit violations
Low load period	CWOA-PAO-MPC	0.95	0.72	1
	GWO-PSO-PID	2.78	1.51	4
	ABC-GA-LQR	2.25	1.18	3
	FA-SA-FLC	1.98	0.98	2
Peak load period	CWOA-PAO-MPC	1.42	0.89	2
	GWO-PSO-PID	4.05	2.59	7
	ABC-GA-LQR	3.42	2.05	5

FA-SA-FLC	2.95	1.65	4

As shown in **Table 1**, under low-load conditions, the power shortage rate of the CWOA-PSO-MPC model was 0.72%, which was 0.26% and 0.79% lower than those of the FA-SA-FLC model and the GWO-PSO-PID model, respectively. Under high-load conditions, the curtailment rate of the CWOA-PSO-MPC model was 1.42%, still much lower than that of the comparison models. The number of unit output exceedances of the CWOA-PSO-MPC model was only two, further demonstrating its constraint satisfaction capability. Overall, the CWOA-PSO-MPC model achieved a balance between economic performance and environmental protection and produced highly reliable scheduling results.

5. Summary and future work

In the development of offshore wind power and the operation of new energy systems, although smart grids provide data and control foundations for energy coordination and low-carbon management, the design of offshore wind power infrastructure has shortcomings such as the difficulty in balancing carbon emissions and costs throughout the entire life cycle. Moreover, current research lacks in-depth exploration of common materials, reactions, and chemical processes in applied chemistry. There is still room for improvement in optimizing infrastructure and new energy systems by integrating applied chemical knowledge. For this purpose, the research proposes the CWOA-PSO-MPC optimization model based on smart grid collaboration. The model utilizes the CWOA improved by chaotic reverse learning to optimize the parameters of the infrastructure and material selection, achieving dual control of carbon emissions and costs. It also combines PSO and MPC to construct a scheduling framework to adapt to output fluctuations and ensure power balance. The experimental results showed that CWOA converged after 100 iterations, with a foundation weight of 3169.3 t, outperforming comparison algorithms such as GWO. Moreover, the CWOA-PSO-MPC model achieved an average cost of 7531.67 dollars, which was lower than those of other models. During high-load periods, the power balance constraint satisfaction rate reached 98.51%, while the power shortage rate during low-load periods was only 0.72%. The model also showed lower power curtailment and fewer unit overload occurrences, effectively balancing economic efficiency, environmental protection, and system stability. However, there are still some limitations in the current research. Firstly, the experimental data is dependent on specific scenarios and fails to cover diverse engineering scenarios such as extreme climates and complex geological conditions. The adaptability and universality of the model need to be further tested. Secondly, the model performs well in handling small-scale system optimization, but when dealing with large-scale multi-energy complementary new energy systems, as the number of variables increases, the algorithm's computational load significantly rises and the real-time response capability declines. Future research will expand the dataset of extreme scenarios, optimize the fitness function and fault-tolerant mechanism, enhance the model's robustness, and introduce lightweight algorithms to compress the number of variables and improve the real-time response capability. This will provide a more comprehensive technical solution for the large-scale development of offshore wind power.

Conflict of interest

The authors declare no conflict of interest.

References

1. He K, Ye J. Seismic dynamics of offshore wind turbine-seabed foundation: Insights from a numerical study[J]. Renewable Energy, 2023, 205: 200-221.
2. Meng X, Zhang Y, Wu Z, et al. Enhancing operations management of pumped storage power stations by partnering from the perspective of multi-energy complementarity[J]. Energies, 2023, 16(19): 7005-7023.
3. Kabeyi M J B, Olanrewaju O A. Smart grid technologies and application in the sustainable energy transition: a review[J]. International Journal of Sustainable Energy, 2023, 42(1): 685-758.

4. Mostafa R R, Hussien A G, Gaheen M A, Ewees A A, Hashim F A. AEOWOA: hybridizing whale optimization algorithm with artificial ecosystem-based optimization for optimal feature selection and global optimization[J]. Evolving Systems, 2024, 15(5): 1753-1785.
5. Liu Y, Lun Q, Zhang J. Dual-objective economic planning of simultaneous allocation of disconnectors and maneuvering points considering the direction of error reduction in the presence of fault detector with the multi-objective PSO[J]. Electrical Engineering, 2025, 107(4): 4021-4036.
6. Wang C, Geng Q, Liu F. Decentralized Event-Triggered Model Predictive Control for Fuzzy Cyber-physical Systems Under Optimal Jamming Attacks[J]. International Journal of Fuzzy Systems, 2025, 27(3): 749-761.
7. Yuan C, Zhang Q, Luo H, et al. Bearing Capacity of Offshore Wind Power Suction Bucket with Supports Under Extreme Wind and Waves[J]. Energies, 2025, 18(10): 2590-2606.
8. Li Y, Yu H, Jiang C, et al. WOA–PSO of fractional-order PID control for arc plasma power supply inverter modules[J]. Journal of Power Electronics, 2025, 25(2): 382-392.
9. Yang Y, Zou L, Cao X, et al. A modified Manson-Halford model based on improved WOA for fatigue life prediction under multi-level loading[J]. International Journal of Damage Mechanics, 2024, 33(10): 774-807.
10. Lu Y, Yang G, Li X, et al. Dynamic power allocation for the new energy hybrid hydrogen production system based on WOA-VMD: Improving fluctuation balance and optimizing control strategy[J]. International Journal of Hydrogen Energy, 2024, 94: 580-599.
11. Zhang H, Wu S, Li H, Zhang J, Zhu C, Zhou H, Jia Y. Multi-Scheme Optimal Operation of Pumped Storage Wind–Solar–Thermal Generation System Based on Tolerable Energy Abandonment[J]. Water, 2024, 16(4): 576-593.
12. Chen Y, Zhang J, Lyu M, et al. Real-time robust nonlinear model predictive control with monotonically increasing weight for quadruped locomotion[J]. Nonlinear Dynamics, 2025, 113(7): 6795-6813.
13. Yang J, Yu D Z. APPSO-NN: An adaptive-probability particle swarm optimization neural network for sensorineural hearing loss detection[J]. IET Biometrics, 2023, 12(4): 211-221.
14. Zhang A, Lin Z, Wang B, et al. Development of a compact rotary series elastic actuator with neural network-driven model predictive control implementation[J]. Intelligent Service Robotics, 2024, 17(3): 641-660.
15. Tang P, Hu J, Feng T, et al. Prediction Model for Shield Tunneling Roll Angle and Pitch Angle: A PCA-PSO-LGBM Approach[J]. APPLIED SCIENCES-BASEL, 2025, 15(5): 2277-2297.